Forced current sheets in a flapping magnetotail

C. M. Cully, R. E. Ergun, E. Lucek, A. Eriksson, D. N. Baker, and C. Mouikis

Abstract: In the late growth phase, a thin current sheet often forms in the magnetotail, with a scale size comparable to the thermal ion gyroradius. This thin current sheet is typically embedded within a much thicker plasma sheet, and often precedes substorm onset. In that sense, it is the initial condition for reconnection or current disruption. A number of models have been developed to explain the equilibrium kinetic solution of such a current sheet. One popular model is the forced current sheet. In this one-dimensional solution, the current is supported by the pressure anisotropy seen in a rapidly translating deHoffmann-Teller frame. In this paper, we search for forced current sheets in the Cluster data from 2001 (at $\sim$19 R_E apogee). First, we develop a forced current sheet model using typical parameters for the magnetotail, including flapping motion. Using this model, we identify the observational characteristics of forced current sheets, concentrating on the DC electric field. We then search for these features in the Cluster data from 2001. Despite searching through more than 100 encounters with stable current sheets, we were unable to find a suitable example. We conclude that the relative velocity between the satellites and the deHoffmann-Teller frame is low, except in extremely dynamic situations. Consequently, forced current sheet models with anisotropy supplied by the deHoffmann-Teller translation are not widely applicable to the stable magnetotail at $\sim$19 R_E.

Key words: Substorms, magnetotail structure, forced current sheets.

1. Introduction

In the past decades, increasingly sophisticated kinetic simulations have been brought to bear on the fundamental processes driving substorms. The impact of these codes has been substantial; for example, the "GEM reconnection challenge" [2] has shaped the way many authors view reconnection. Nonetheless, the utility of these simulations depends on finding the correct initial and boundary conditions.

Some simulations are relatively insensitive to the initial conditions. For example, the GEM challenge imposes a rather extreme perturbation at the boundary, which forces the reconnection to develop in a manner relatively insensitive to the initial conditions. The reasoning is that these simulations focus on the basic plasma physics, and the development from initial conditions is not of interest.

The magnetosphere probably doesn't supply such radical boundary conditions, and the processes that occur within are thus more influenced by initial conditions. Several authors have noted that the magnetotail exhibits hysteresis [15, 26], which is a dramatic example of sensitivity to initial conditions. We feel that it is important to understand the stable equilibrium of the magnetotail.

Most simulations use a Harris model [10] for the initial condition. While simple and attractive, the Harris model is one dimensional and does not include the observed normal component of the magnetic field (B_z). Some authors simply add a constant normal component to construct a field geometry more consistent with observations. However, the magnetic tension force in the resulting configuration is unbalanced, resulting in a non-equilibrium state.

More complicated equilibrium solutions do exist. One major class of equilibrium solutions assumes an isotropic distribution, and allows the plasma parameters to vary across field lines [13, 18, 21, 22]. In this paper, we will not focus on these 2-dimensional models.

A second major class of solutions assumes anisotropic distributions ($P_{||} > P_{\perp}$) at the model boundaries [6–8, 12, 25, 28]. Known as forced current sheet models, this class of solutions is entirely one-dimensional. In this paper, we try to better understand the applicability of forced current sheets at Cluster apogee ($\sim$19 R_E).

Our first task is to extend some of the numerical simulations of forced current sheets [6]. One of the key discoveries of the Cluster mission is extensive spatial structure in the $\pm$y direction, often seen as even-parity (kink-type) oscillations [20, 23]. Indeed, since this flapping is what usually causes the satellites to pass through the current sheet, the vast majority of observations occur during intervals of flapping. Consequently, the particular extension we are interested in is this: what happens to a forced current sheet if wave structure develops in the current-carrying ($\pm$y) direction?

After developing the model, we are in a position to assess how much forcing is required to drive these models in realistic circumstances (i.e. how large of an electric field). We then use this knowledge to search for an example of a forced current sheet in the Cluster data from 2001.

The first section of this paper is a review of the basics of forced current sheet models. The second section extends the models to situations with kink-type structure in the y direction, and quantifies how much forcing is required. After a brief comparison of the required forcing to previously-published average conditions, we then describe a search for these conditions using Cluster data from 2001. The results of the search are negative: we were unable to find an example of a forced current sheet.

Received 5 June 2006.

C. M. Cully, R. E. Ergun, and D. N. Baker. Laboratory for Atmospheric and Space Physics, University of Colorado, Boulder, USA.
E. Lucek. Space and Atmospheric Physics Group, Imperial College, London, UK.
A. Eriksson. Swedish Institute of Space Physics, Uppsala, Sweden.
C. Mouikis. Department of Physics, University of New Hampshire, USA.

2. Forced Current Sheets

Forced current sheets are sheet configurations in which the magnetic field is supported by an anisotropic plasma pressure. There is an extensive literature that discusses these models, from early work in the 1970's [12,19] to recent work published in the past few months [31].

Consider a current sheet in the $\hat{y}$ direction, with the sheet normal to $\hat{z}$, as sketched in Figure 1. The resulting magnetic field reverses sign at $z = 0$, and there is an additional constant normal component B_z (assumed positive). The sheet is connected at large values of z (both positive and negative) to a reservoir of particles. Because of the normal component B_z, particles may flow along the field lines and interact with the sheet, either crossing it to flow into the reservoir on the other side, or reflecting back to the initial reservoir.

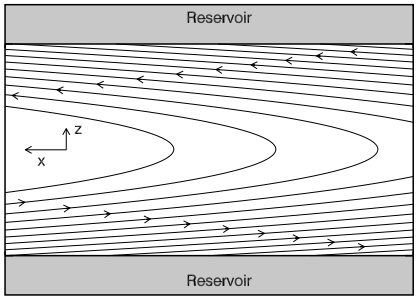

Fig. 1. Magnetic field configuration and coordinate system. $\hat{y}$ is out of the page.

The essential idea for a forced current sheet is that particles in the reservoirs have a larger parallel pressure than perpendicular pressure. Their parallel velocities are initially to the right in Figure 1, and are bent back to the left by their interaction with the sheet. They consequently exert a reaction force on the sheet in the negative $\hat{x}$ direction. Equilibrium is achieved when this force exactly balances the magnetic tension force.

The pressure anisotropy in the reservoir is generally assumed to arise from one of two conditions. Either the parallel temperature is larger than the perpendicular temperature, or the distribution flows along the field line with some parallel velocity. A combination of these two conditions is also possible. Early formulations tended to focus on the first possibility, while more recent works [6, 25, 28] focus on the second possibility: large parallel flow. The term "forced current sheet" was coined by Burkhart et al., and applies principally to this second condition [6].

Parallel flow might at first seem to be an unlikely candidate to support a quiet-time current sheet, since satellite observations seldom show the near-Alfvénic flows required. However, the relevant frame in which to assess the pressures is the deHoffmann-Teller frame. If the normal magnetic field B_z is small, then a small convection field E_y can cause the deHoffmann-Teller frame to translate very rapidly in the $\hat{x}$ direction. For example, a convection electric field E_y=1 mV/m combined with a constant normal field B_z=2 nT creates a deHoffmann-Teller frame moving at 500 km/s. Near the particle reservoirs at the edges, this motion is very nearly parallel to $\vec{B}$.

The maximum current that can be generated from an anisotropic distribution is given by the marginal firehose criterion [12, 19]:

$$\frac{B^2}{\mu_0} = P_{||} - P_{\perp} \tag{1}$$

where both the magnetic field B and the pressures $P_{||}$ and $P_{\perp}$ are taken at the boundary, far from the sheet. The pressures are functions of both the conditions at the reservoir (which determines the incoming half of the distribution function) and the current sheet itself (which determines the outgoing half).

In the case where the excess parallel pressure is supplied by a parallel drift V_D at the boundary, and in the limit of zero pitch angle scattering by the sheet, the marginal firehose condition reduces simply to $V_D = V_A$, the Alfvén speed far from the sheet. In the other limit, that of perfect isotropization by the sheet, a larger speed is required: $V_D = \sqrt{3}V_A$ [6].

The drift speed V_D is related to the deHoffmann-Teller speed V_{HT} by the relation $V_D = V_{HT}\cos(\theta)$, where θ is the (small) inclination angle of the asymptotic field $\theta = \tan^{-1}(B_z/B_x)$ with B_x and B_z evaluated at the boundary. The drift is strictly parallel to $\vec{B}$ in the deHoffmann-Teller frame, as required by the condition that the electric field vanish.

The marginal firehose condition is, however, only an upper bound on the possible current. Numerical simulation [6] has shown that this maximum current is attained for sufficiently thin sheets. "Sufficiently thin" in this case can be assessed using the parameter

$$\kappa = \sqrt{\frac{R_{\min}}{\rho_{\max}}} \tag{2}$$

where $R_{\min}$ is the minimum radius of curvature of the field line and $\rho_{\max}$ is the maximum Larmor radius of a thermal-energy ion [4]. In order to reach the marginal firehose limit, κ must be less than about 0.2 [6]. In this regime, the sheet is sufficiently thin that the ions execute Speiser-type orbits [29].

For values of κ between roughly 0.2 and 0.7, a forced current sheet still develops, but with a smaller magnetic field (closer to the lower limit $V_D = \sqrt{3}V_A$). No solutions have been found for values of κ above 0.7. This condition marks the onset of deterministic chaos in the particle trajectories [4]. It has been proposed [6] that no equilibrium solution exists in this chaotic range $\kappa \approx 1$, and that a sheet that approaches this condition may suffer a catastrophic loss of equilibrium.

Assuming a small value of κ ($\lesssim 0.2$), the quasi-adiabatic invariant

$$I_z = \frac{1}{2\pi}\oint mv_z \mathrm{d}z \tag{3}$$

is approximately conserved [24]. An elegant analytical model [25] can be created by explicitly conserving this quantity. This extends the applicability of the forced current sheet models into the regime $V_D \lesssim V_T$ (with V_T the thermal velocity). This regime is difficult to access with numerical studies due to poor signal-to-noise ratio. With the assumption $\kappa \ll 1$, the marginal firehose condition gives the appropriate field magnitude (not just an upper bound).

3. Numerical Investigation

The numerical model we chose is an iterative self-consistent method fundamentally similar to the one used by Burkhart et al. [5, 6]. The method treats the full motion of the ions, but treats the electrons as a charge-neutralizing fluid using a simple Boltzmann approximation. Ions are initially traced through trial electric and magnetic fields, with the resulting velocity and density moments calculated on a grid. New fields are then computed using these moments, and the particles are traced through these new fields. This process is repeated until the fields converge from one iteration to the next (or diverge – see below).

The simulation box in our study is a 256 by 256 element rectangular domain in the y-z plane. We initialize ions at the top and bottom edges of the domain according to a drifting Maxwellian distribution. The drift is parallel to the magnetic field, as required in the deHoffmann-Teller frame. Particles are then traced in three dimensions through the simulation box using the non-relativistic Lorentz force equation. We use a fourth-order adaptive-stepsize Runge-Kutta integrator, and 20000 to 100000 particles per iteration.

The magnetic field on the first iteration is given by an initial guess as a hyperbolic tangent with an asymptotic field strength given by the marginal firehose condition and a constant normal component B_{z0}. On subsequent iterations, we find the magnetic field by

$$\vec{B} = \nabla \times \vec{A} + B_{z0}\hat{z} \quad (4)$$

$$\nabla^2 \vec{A} = -\mu_0 n(y,z)\vec{v}(y,z) \quad (5)$$

$$(6)$$

where B_{z0} is a constant and all other symbols have their usual meanings. Velocities and densities are computed directly from the particle distributions at each grid point. Velocities in the x direction are small, and we do not include them in the calculation of the magnetic field.

The electric field is initially set to zero. On subsequent iterations, we calculate it by

$$\vec{E} = -\nabla\phi + \vec{E}_{\rm external} \quad (7)$$

$$\frac{e\phi(y,z)}{kT_e} = \ln\left(\frac{n(y,z)}{n_0}\right) \quad (8)$$

$$(9)$$

where T_e is the electron temperature and n_0 is the average density at the top boundary. The results are relatively independent of the electron temperature, as noted previously [6].

Convergence for this method typically takes only a few iterations. It indicates the existence of a time-stationary solution, but does not guarantee stability. Some of the distribution functions encountered both in this work and in the other forced current sheet literature are clearly unstable to a variety of instabilities. Assessing this is, however, outside the scope of this article.

Divergence typically occurs for one of two reasons. First, when the drift speed is small relative to the thermal speed ($V_D \lesssim V_T$), numerical noise becomes a problem. This can be remedied by simply adding more particles, and has no physical relevance. Second, the method diverges when the κ parameter (equation 2) is larger than $\sim$0.7. As discussed above, it seems likely that no stationary solution can exist in this chaotic range, in which case the method diverges for physically meaningful reasons [6].

We report here on two simulation runs. In the first run, we used a flat sheet with no electric field E_y, a normal component of the magnetic field B_{z0} = 2 nT and a density n_0 of 0.3 cm^{-3}. The thermal speed of the incoming distribution was 600 km/s (i.e. 1.9 keV), and we varied the (parallel) drift speed up to 2000 km/s. The asymptotic magnetic field far from the resulting current sheet is shown as the filled circles in Figure 2.

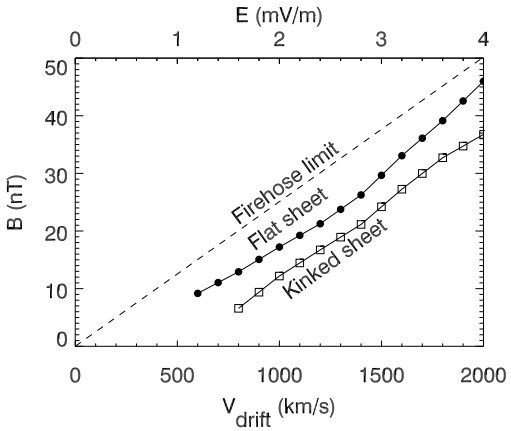

Fig. 2. Maximum magnetic field as a function of drift velocity V_D, for a flat sheet and a sheet with a kink-type wave. Equivalent electric fields in the 2 nT normal magnetic field are shown on the upper abscissa.

Setting the electric field to zero puts the simulations in the deHoffmann-Teller frame. An equivalent simulation was also performed in the drifting frame, with the drift velocity set to zero and the external electric field varied. The results of the two techniques are consistent.

At larger values of the drift velocity V_D, the magnetic field asymptotes to the marginal firehose limit. However, at more realistic values of V_D, the finite temperatures of both the ions and the electrons (T_e=400 eV) cause the sheet to thicken. The wider sheet increases the value of κ enough that increased pitch angle scattering occurs, and the magnetic field is closer to the strong-scattering limit of $1/\sqrt{3}$ times the marginal firehose limit.

The second set of simulations used the same parameters, except that we introduced an even parity (kink-type) wave structure into the sheet. The waves were supported by an electric field

$$E_y = -\omega a B_x \cos(ky) \quad (10)$$

with ω, a and k the wave frequency, amplitude and wavenumber respectively. This is the induced electric field

$$\nabla \times \vec{E} = -\frac{\partial B}{\partial t} \quad (11)$$

caused by a changing magnetic field

$$B_x(y,z,t) = B_x(z') \quad (12)$$
$$z' = a\sin(ky - \omega t) \quad (13)$$

in the rest frame. The introduced wave had a period of 60 seconds, an amplitude of 500 km and a wavelength of 7500 km. We implicitly assume here that a stable, non-growing kink-type mode exists. While observationally reasonable (see section 5), we cannot verify this stability with the current model.

This induced field is not curl-free, and cannot be transformed away. That is, no deHoffmann-Teller frame exists under these conditions. This isn't a problem in the simulations, since the physics is independent of the frame, and the simulation frame can be switched easily. However, since the method is time-independent, there is one restriction on the frame: it must be co-moving in $\hat{y}$ with the wave. In the frame moving at $\vec{c}_{\rm frame} = (\omega/k)\hat{y}$, an additional electric field $\vec{E}' = \vec{c}_{\rm frame} \times \vec{B}$ arises from the Galilean transformation. Since the solution in this co-moving frame is time-independent, the numerical method is applicable without the need to extend to the time domain.

The numerical technique converges for roughly the same range of parameters as the flat sheet. Although the familiar caveats apply regarding the stability of the solution, this means that we have found an equilibrium solution with a kink-type wave present. Figure 3 is a pair of contour plots of the converged solution for V_D=2000 km/s. Shown are the density and velocity. The sheet is roughly 700 km across, with a strong density peak near the centre. Lower drift speeds result in a broader sheet (up to twice as thick) with a less-pronounced density maximum. The velocity enhancement is somewhat wider than the density enhancement. The direction of the velocity vectors closely follows the kink motion.

The asymptotic magnetic field for this simulation run is plotted using open squares in Figure 2. For the same drift speed, the structured current sheet does not support as much current. The reason for this behaviour seems to be that the kinked sheet randomizes the trajectories more than the flat sheet. This widens out the sheet (by about a factor of 2) and reduces the total current.

The goal of these numerical studies is to estimate the minimum electric field required to support a forced current sheet under realistic conditions. Referring to Figure 2, it's clear that for a typical 25 nT asymptotic field, the electric field must be at least 2 mV/m in a sheet with a density of 0.3 cm^{-3}.

4. Comparison to published averages

In the satellite frame, the anisotropy required for a forced current sheet could manifest itself in three different ways. A large anisotropy in the ion distribution is one fairly obvious signature. Observationally, however, the required anisotropies are rarely observed [17, 22]. Typical observed anisotropies in the current sheet are substantially less than 10% [14]. Assuming a typical pressure of 0.2 nPa at 20 R_E [14], a 10% anisotropy results in a maximum field strength of only 5 nT (using the marginal firehose condition). While certainly possible in extremely dense sheets, or under conditions of unusually large anisotropy, it seems unlikely that the temperature anisotropy could frequently support forced current sheets.

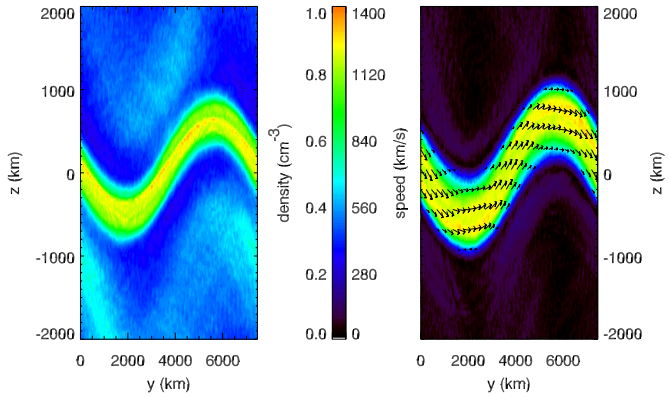

Fig. 3. Density (left) and speed (right) for a forced current sheet with a kink-type wave. Selected velocity vectors have been plotted in the right hand panel.

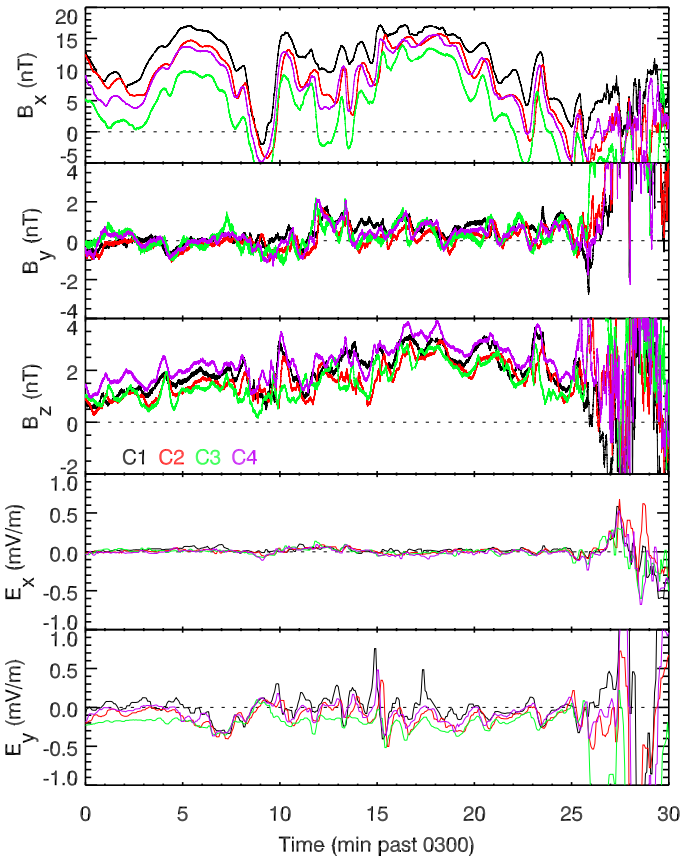

Fig. 4. Cluster magnetic and electric field data from 2001 October 11. Colour coding is black, red, green, magenta for Cluster satellites 1 through 4 respectively (see panel 3).

A second possibility is that the anisotropy could manifest itself as a bulk flow in the spacecraft frame. With typical bulk flows less than 50 km/s [14], this translates to no more than a few nT.

The final possibility is that the deHoffmann-Teller frame is translating rapidly with respect to the spacecraft frame. Typical electric fields are roughly 0.2 mV/m [30], which when coupled

with a normal magnetic field of some 2 nT results in a 100 km/s drift. Again using typical parameters, this yields only a ± 5 nT asymptotic magnetic field.

From the statistical observations, it seems fair to conclude that the average magnetotail is not described by a forced current sheet model. On the other hand, thin current sheets are not "statistically average" events. Indeed, large anisotropies have occasionally been observed prior to substorm onset [16]. Consequently, we decided to re-examine the observations to search for forced current sheets.

5. Case study

Figure 4 shows Cluster observations of a stable current sheet encounter on October 11^{th} 2001, immediately prior to a substorm. The top three panels display the magnetic field from the FGM fluxgate magnetometer [1] in a coordinate system chosen to match the simulation coordinates. The current sheet normal $\hat{z}$ was found at each data point as the gradient [11] in the magnetic field strength. The coordinate system for Figure 4 uses the average $\hat{z}$ direction, and $\hat{x}$ was found by rotating about this axis to maximize the field in x and minimize the field in y.

Between 0310 UT and 0320 UT, there are strong waves that rotate the sheet normal $\hat{z}$ by roughly 60 degrees. The mode is largely even parity (kink-type), as evidenced by the fact that the oscillations at C3 remain in phase even when B_x is negative (i.e. the satellite is on the opposite side of the sheet). Timing analysis on the oscillations gives a phase velocity of $\sim$120 km/s in the $\hat{y}$ direction. With the 60 second period, this gives a wavelength of 7200 km. Using this wavelength, the 60 degree rotation of $\hat{z}$ implies an amplitude of 500 km.

The amplitude can be independently verified by noting the satellite separation in z. Cluster 3 is lowest in z, followed by C4, then C2, and C1 is highest. The relative z separations are 893 km, 1061 km and 1986 km respectively. Since the top of the C3 trace barely overlaps with the C2 and C4 traces, which in turn barely overlap with the C1 trace, the amplitude must be roughly half the separation distance, or $\sim$500 km. The embedded sheet thickness can also be estimated in this manner as something like 2500 km.

At 0325 UT, the current sheet begins to rapidly break up. On the ground, there is evidence of a pseudobreakup at this time; the main substorm follows after that. For this study, however, we're interested more in the interval before this happens.

The bottom two panels show the electric field from the Cluster EFW double-probe electric field instrument [9] in the same rotated coordinate system. Cluster EFW only measures in two dimensions: roughly $\hat{x}$ and $\hat{y}$. To project to this system, we have assumed zero electric field along the unmeasured axis. An offset has also been subtracted from the sunward direction ($\sim \hat{x}$).

As a check on the assumption that the unmeasured component is roughly zero, we tried determining it using the constraint $\vec{E} \cdot \vec{B} = 0$. This yielded similar results, except when $\vec{B}$ was near the spin plane (in which case this second method has a well known divide-by-zero failure).

There is a clear oscillation in E_y. It has the same period as the magnetic kink-mode oscillations, but is 90 degrees out of phase. Applying equation 10, the induced electric field in the y direction should be ~ 0.2 mV/m for kink-mode oscillations with the characteristics found above, and should be 90 degrees out of phase. Consequently, we interpret these oscillations as resulting from the same even-parity perturbation to the sheet.

In summary, kink-type waves are clearly seen, and the electric field measurements resolve the ~ 0.2 mV/m fields from this motion. What is notably lacking, however, is any evidence of a strong DC electric field. The field is much less than the > 2 mV/m that would be required for this to be a forced current sheet. There is also little anisotropy in the particle measurements (not shown). This is clearly not an example of a forced current sheet.

6. Event search

We tried to find an example of a stable forced current sheet driven by DC electric fields in the 2001 Cluster data. Based on the results shown in Figure 2, the required electric field is

$$E_y \gtrsim (2\mathrm{mV/m})\sqrt{\frac{0.3\mathrm{cm}^{-3}}{n}}\left(\frac{B_z}{2\mathrm{nT}}\right). \quad (14)$$

In order to include as many events as possible, we looked for stable sheets that had E_y greater than half this value. Despite looking at more than 100 stable current sheets, no events were found.

There were certainly intervals in the Cluster data when E_y exceeded this threshold. However, these were invariably in extremely dynamic, unstable current sheets. The portion of the event shown in Figure 4 after 0325 UT is an example.

7. Conclusions

We used an iterative self-consistent method to find a stationary solution for a forced current sheet with a kink-type wave. This is the first report of this type of solution. The solution is similar in many ways to the solution for a flat forced current sheet, except that the sheet is considerably thicker. This thicker sheet translates into a reduced efficiency for converting the pressure anisotropy into an organized current.

We estimated the electric field required to establish a forced current sheet with equal parallel and perpendicular pressures in the satellite frame. The result was quite large: at least 2 mV/m in typical sheets.

We then searched the Cluster data for 2001 for an example of a stable forced current sheet supported by a DC electric field, either with or without kink-type structure. Our failure to find an example means that the relative velocity between the satellite frame and the deHoffmann-Teller frame is low, except in extremely dynamic situations. We conclude that forced current sheet models (with anisotropy supplied by the deHoffmann-Teller translation) are not widely applicable to the stable magnetotail at $\sim$19 R_E.

This does not mean that these models are never applicable. However, it does restrict their domain. First, they could be useful in very dynamic situations with large DC electric fields. This is an important class of phenomena including reconnection outflow regions and bursty bulk flows. Second, periods of unusually large pressure anisotropy do exist. A follow-on study searching for such events would be worthwhile.

8. Acknowledgments

We thank Melvyn Goldstein for PEACE data and useful discussions. The FGM data were accessed through the Cluster Active Archive. This work was supported by THEMIS (Time History of Events and Macroscale Interactions during Substorms).

References

1. Balogh, A., Carr, C.M., Acuña, M.H., Dunlop, M.W., Beek, T.J., Brown, P., Fornacon, K.-H., Georgescu, E., Glassmeier, K.-H., Harris, J., Musmann, G., Oddy, T., and Schwingenschuh, K., The Cluster Magnetic Field Investigation: overview of in-flight performance and initial results, *Ann. Geophysicae, 19*, 1207-1217, 2001.
2. Birn, J., Drake, J.F., Shay, M.A., Rogers, B.N., Denton, R.E., Hesse, M., Kuznetsova, M., Ma, Z.W., Bhattacharjee, A., Otto, A., and Pritchett, P.L., Geospace Environmental Modeling (GEM) magnetic reconnection challenge, *J. Geophys. Res., 106*, 3715–19, 2001.
3. Birn, J., Galsgaard, K., Hesse, M., Hoshino, M., Huba, J., Lapenta, G., Pritchett, P.L., Schindler, K., Yin, L., Büchner, J., Neukirch, T., and Priest, E.R., Forced magnetic reconnection, *Geophys. Res. Lett., 32*, L06105, 2005.
4. Büchner, J., and Zelenyi, L., Regular and chaotic charged particle motion in magnetotaillike field reversals 1. Basic theory of trapped motion, *J. Geophys. Res., 94*, 11,821–11,842, 1989.
5. Burkhart, G.R., Drake, J.F., and Chen, J., The structure of the dissipation region during magnetic reconnection in collisionless plasma, *J. Geophys. Res., 96*, 11,539–53, 1991.
6. Burkhart, G.R., Drake, J.F., Dusenbery, P.B., and Speiser, T.W., A particle model for magnetotail neutral sheet equilibria, *J. Geophys. Res., 97*, 13,799-815, 1992.
7. Eastwood, J.W., Consistency of fields and particle motion in the Speiser model of the current sheet, *Planet. Space Sci., 20*, 1555, 1972.
8. Eastwood, J.W., The warm current sheet model, and its implications on the temporal behaviour of the geomagnetic tail, *Planet. Space Sci., 22*, 1641, 1974.
9. Gustafsson, G., Boström, R., Holback, B., Holmgren, G., Lundgren, A., Stasiewicz, K., Åhlén, L., Mozer, F.S., Pankow, D., Harvey, P., Berg, P., Ulrich, R., Pedersen, A., Schmidt, R., Butler, A., Fransen, A.W.C., Klinge, D., Thomsen, M., Fälthammar, C.-G., Lindqvist, P.-A., Christenson, S., Holtet, J., Lybekk, B., Sten, T.A., Tanskanen, P., Lappalainen, K., and Wygant, J., The electric field and wave experiment for the Cluster mission, *Space Science Reviews, 79*, n 1-2, 137-56, 1997.
10. Harris, E.G., On a plasma sheet separating regions of oppositely directed magnetic fields, *Nuevo Cimento, 23*, 115, 1962.
11. Harvey, C.C., Spatial gradients and the volumetric tensor, *in Analysis Methods for Multispacecraft Data*, edited by G. Paschmann and P.W. Daly, 307–322, ISSI, Bern, 1998.
12. Hill, T.W., Magnetic merging in a collisionless plasma, *J. Geophys. Res., 80*, 4689, 1975.
13. Kan, J.R., On the structure of the magnetotail current sheet, *J. Geophys. Res., 78*, 3773, 1973.
14. Kaufmann, R.L., Paterson, W.R., Frank, L.A., Relationships between the ion flow speed, magnetic flux transport rate, and other plasma sheet parameters, *J. Geophys. Res., 110*, A09216, 2005.
15. Klimas, A.J., Uritsky, V.M., Vassiliadis, D., Baker, D.N., Reconnection and scale-free avalanching in a driven current-sheet model, *J. Geophys. Res., 109*, A02218, 2004.
16. LeContel, O., Perraut, S., Roux, A., Pellat, R., and Korth, A., Substorms in the inner plasma sheet, *Adv. Space Res., 25*, 2395–2406, 2000.
17. Nötzel, A., Schindler, K., and Birn, J., On the cause of the approximate pressure isotropy in the quiet near-Earth plasma sheet, *J. Geophys. Res., 90*, 8293–300, 1985.
18. Pritchett, P.L., and Coroniti, F.V., Formation of thin current sheets during plasma sheet convection, *J. Geophys. Res., 100*, 23,551-65, 1995.
19. Rich, F.J., Vasyliunas, V.M., and Wolf, R.A., On the balance of stresses in the plasma sheet, *J. Geophys. Res., 77*, 4670, 1972.
20. Runov, A., Nakamura, R., Baumjohann, W., Zhang, T.L., Volwerk, M., and Eichelberger, H.-U, Cluster observation of a bifurcated current sheet, *Geophys. Res. Lett., 30*, 1036, 2003.
21. Schindler, K., Pfirsch, D., and Wobig, H., Stability of two-dimensional collison-free plasmas, *Plasma Phys., 15*, 1165, 1973.
22. Schindler, K., and Birn, J., Models of two-dimensional embedded thin current sheets from Vlasov theory, *J. Geophys. Res., 107*, 1193, 2002.
23. Sergeev, V., Runov, A., Baumjohann, W., Nakamura, R., Zhang, T.L., Volwerk, M., Balogh, A., Rème, H., Sauvaud, J.A., André, M., and Klecker, B., Current sheet flapping motion and structure observed by Cluster, *Geophys. Res. Lett., 30*, 1327, 2003.
24. Sonnerup, B.U.O., Adiabatic particle orbits in a magnetic null sheet, *J. Geophys. Res., 76*, 8211, 1971.
25. Sitnov, M.I., Zelenyi, L.M., Malova, H.V., and Sharma, A.S., Thin current sheet embedded within a thicker plasma sheet: self-consistent kinetic theory, *J. Geophys. Res., 105*, 13029-43, 2000.
26. Sitnov, M.I., Sharma, A.S., Papadopoulos, K., and Vassiliadis, D., Modeling substorm dynamics of the magnetosphere: From self-organization and self-organized criticality to nonequilibrium phase transitions, *Physical Review E - Statistical, Nonlinear, and Soft Matter Physics, 65*, 016116, 2001.
27. Sitnov, M.I., Guzdar, P.N., and Swisdak, M., A model of the bifurcated current sheet, *Geophys. Res. Lett., 30*, 1712, 2003.
28. Sitnov, M.I., Lui, A.T.Y., Guzdar, P.N., and Yoon, P.H., Current-driven instabilities in forced current sheets, *J. Geophys. Res., 109*, A03205, 2004.
29. Speiser, T.W., Particle trajectories in model current sheets, 1, Analytical solutions, *J. Geophys. Res., 70*, 4219, 1965.
30. Wang, C-P., Lyons, L.R., Weygand, J.M., Nagai, T., and McEntire, R.W., Equatorial distributions of the plasma sheet ions, their electric and magnetic drifts, and magnetic fields under different interplanetary magnetic field B_z conditions, *J. Geophys. Res., 111*, A04215, 2006.
31. Zelenyi, L.M., Malova, H.V., Popov, V.Y., Delcourt, D.C., Ganushkina, N.Y., and Sharma, A.S., "Matreshka" model of multilayered current sheet, *Geophys. Res. Lett., 33*, L05105, 2006.